High-precision prompt-γ-ray spectral data from the reaction ^{241}Pu(n_{th}, f)

S. Oberstedt,[1,*] R. Billnert,[1,2] T. Belgya,[3] T. Bryś,[1] W. Geerts,[1] C. Guerrero,[4,5] F.-J. Hambsch,[1] Z. Kis,[3] A. Moens,[1]
A. Oberstedt,[2,6] G. Sibbens,[1] L. Szentmiklosi,[3] D. Vanleeuw,[1] and M. Vidali[1]

[1]*European Commission, Joint Research Centre (IRMM), B-2440 Geel, Belgium*
[2]*Fundamental Fysik, Chalmers Tekniska Högskola, S-41296 Göteborg, Sweden*
[3]*Centre of Energy, Institute for Energy Security and Environmental Safety (EKBI), HAS, H-1525 Budapest POB 49, Hungary*
[4]*CERN Physics Department, CH-1211 Genève 23, Switzerland*
[5]*Universidad de Sevilla, Facultad de Fisica, 41012 Sevilla, Spain*
[6]*OSSOLUTIONS Consulting, S-70353 Örebro, Sweden*
(Received 3 February 2014; published 26 August 2014)

In this paper we present results from the first high-precision prompt-γ-ray spectral measurements from the reaction ^{241}Pu(n_{th}, f). Apart from one recent experiment, no data are reported in the literature for this fissioning system, which motivated a new dedicated experiment. We have measured prompt-fission γ rays with three cerium-doped LaBr$_3$ (two 5.08 cm × 5.08 cm and one 7.62 cm × 7.62 cm) and one CeBr$_3$ (5.08 cm × 5.08 cm) scintillation detectors, which all exhibit excellent timing and good energy resolution. The average γ-ray multiplicity was determined to be $\overline{\nu}_\gamma = (8.21 \pm 0.09)$ per fission, the average energy to be $\epsilon_\gamma = (0.78 \pm 0.01)$ MeV, and the total energy to be $E_{\gamma,\text{tot}} = (6.41 \pm 0.06)$ MeV as the weighted average from all detectors. Since the results from all detectors are in excellent agreement, and the total released γ energy is modestly higher than the one in the present evaluated nuclear data files, we suspect that the underestimation of the prompt-γ heating in nuclear reactors is due to fast-neutron-induced fission on ^{238}U or rather from fission induced by γ rays from neutron capture in the construction material.

I. INTRODUCTION

In recent years the measurement of prompt-fission γ-ray spectra (PFGS) has gained renewed interest [1–3], after about forty years since the first comprehensive studies of the reactions ^{235}U(n_{th}, f) [4–6] and ^{252}Cf(sf) [4]. These new experimental efforts were motivated by requests for new values, especially for γ-ray multiplicity and mean photon energy release per fission in the thermal-neutron-induced fission of ^{235}U and ^{239}Pu [7]. Both isotopes are considered the most important ones with respect to the modeling of innovative cores required for fast generation-IV reactors [8–10]. Discrepancies observed in various benchmarks for the calculated total γ heating relative to the measured one range from 10% to 28% [11,12], whereas an accuracy of 7.5% is requested. As a consequence of recent instrumental advancements like the development of new detectors as well as digital data-acquisition systems, the determination of new and improved PFGS characteristics became possible with high precision. An example is a recent study on PFGS from the spontaneous fission of ^{252}Cf and the thermal-neutron-induced fission on ^{235}U (cf. Refs. [1,2], and references therein). The latter showed that the total prompt-γ-ray energy released in fission was underestimated in ENDF/B-VII.1 [13] by about 5%. Since the evaluation for this isotope is based on the

experimental data of Verbinksi *et al.* from 1973 [4], one may expect that an underestimation in the evaluation of the PFGS data for ^{239}Pu is of a similar order of magnitude. All together, this led us to the assumption that the 10% to 28% underestimation of the total prompt-γ heat cannot be explained by an insufficient quality of the historical data. We suspect that other isotopes, present in the nuclear fuel, contribute to the observed underestimation. One candidate could be the fissile plutonium isotope ^{241}Pu or the fertile ^{238}U. Both evaluations seem to be scaled *copies* from the evaluated data file for the PFGS from neutron-induced fission on ^{239}Pu and from the spontaneous fission of ^{252}Cf, respectively. For the latter we had already found an underestimation of the total energy release by about 9%.

Parallel to advancements in experimental techniques, new and refined computer codes were developed both at CEA Cadarache [14,15] and by a collaboration between the Los Alamos National Laboratory and the Rensselaer Polytechnic Institute [16,17], which simulated prompt-neutron and γ-ray emission from primary fission fragments by a Monte Carlo approach together with a full Hauser–Feshbach calculation. Both theoretical models not only describe well the spectral shape of the continuous prompt-γ-ray spectra, but also reproduce also the discrete γ peaks observed experimentally below 1 MeV photon energy (see, e.g., Refs. [1,2]). These very detailed features allow a serious comparison of the deduced PFGS characteristics like photon multiplicity and average and total photon energy per fission with experimentally found values, if experiments provide the same amount of detailed information as given by the calculations mentioned above. The recent work on ^{235}U showed that this is indeed possible [2].

Based on our experience [1,2] we performed a high-precision measurement of thermal-neutron-induced prompt-fission γ rays from ^{241}Pu, which is reported below.

II. EXPERIMENTS, SAMPLE CHARACTERISTICS, AND DATA TREATMENT

The experiment was carried out in June 2013 with the cold-neutron beam of the 10 MW research reactor of the Budapest Neutron Centre [18], Hungary, in order to measure prompt-fission γ rays from the reaction $n_{th} + {}^{241}$Pu. In the following we always refer to thermal-neutron-induced fission, because we believe that the difference between thermal and cold in terms of excitation energy of the fissioning nucleus is negligible. Two plutonium samples were exposed to the cold-neutron beam and γ rays were measured in coincidence with fission fragments as described below in more detail. The thermal-neutron equivalent flux at the sample position was about 5×10^7 neutrons cm^{-2} s^{-1}. In total, 4.2×10^7 prompt-fission γ rays were registered in about 160 h.

The plutonium samples were made at the Institute for Reference Materials and Measurements (IRMM). A plating cell with a rotating platinum anode was used. This cell was specifically designed and produced at IRMM from polyacetal. Plutonium oxide was deposited on a 25-μm-thick Al foil as a circular spot with diameter (19.99 ± 0.01) mm. This Al foil was mounted on an Al ring with an inner diameter of 30 mm and an outer diameter of 40 mm. Mass and areal density of the ^{241}Pu layer were calculated from the ^{241}Pu alpha activity measured by means of α-particle counting with a well-defined solid angle. Prior to molecular plating, the plutonium batch was radio-chemically purified from present decay products, mainly ^{241}Am. The final isotopic composition of the plutonium material was measured by means of thermal-ionization mass spectrometry and is summarized in Table I. From this table it can be deduced that the thermal-neutron-induced fission cross-section weighted contribution from ^{239}Pu in the spectra is smaller than 10^{-5}.

Two plutonium samples with areal mass densities of (12.66 ± 0.12) μg/cm^2 and (13.53 ± 0.17) μg/cm^2 were placed inside a twin-Frisch-grid ionization chamber in back-to-back geometry on the center of the cathode electrode, which delivered the fission trigger. Due to the thick Al foil, only one fission fragment was detected for each fission event. The fission rate was about 5 kHz per sample.

TABLE I. Summary of the isotopic composition of the plutonium targets on March 22, 2013, 12:00 UTC + 01:00. The uncertainties for the mass fractions are expanded combined standard uncertainties, coverage factor $k = 2$.

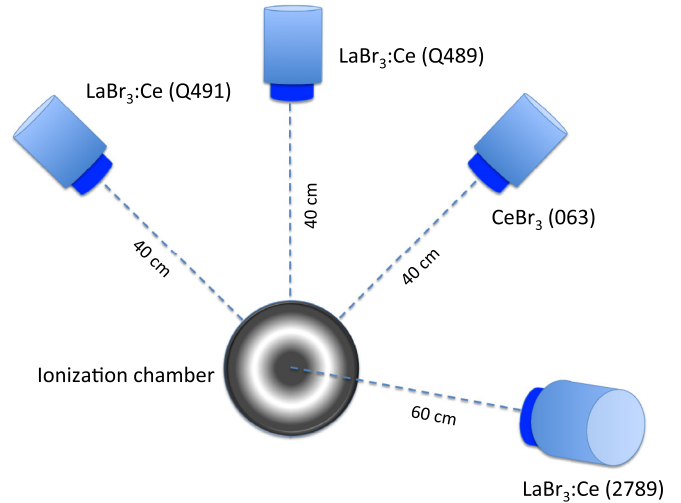| Isotope	Mass fraction
^{238}Pu	0.0000080 (*84*)
^{239}Pu	0.000012 (*13*)
^{240}Pu	0.002431 (*28*)
^{241}Pu	0.993370 (*32*)
^{242}Pu	0.00417960 (*64*)
^{244}Pu	0.0000001 (*15*)

FIG. 1. (Color online) Sketch of the prompt-fission γ-ray-measurement setup: two LaBr$_3$:Ce detectors and one CeBr$_3$ detector, all of size (diameter $\times$ length) 5.08 cm $\times$ 5.08 cm, were placed at 90 degrees relative to the neutron-beam axis at a distance of 40 cm from the plutonium sample. The fourth detector, a LaBr$_3$:Ce with dimensions 7.62 cm $\times$ 7.62 cm, was placed at about 30 degrees relative to the neutron-beam axis and 60 cm away from the fission source.

The coincident measurement of photons was accomplished with four lanthanide halide detectors simultaneously. Two coaxial LaBr$_3$:Ce and one coaxial CeBr$_3$ scintillation detectors with 5.08 cm $\times$ 5.08 cm (diameter $\times$ length) crystals were placed at 90 degrees relative to the neutron-beam axis at a distance of 40 cm. The properties of the lanthanide halide detectors used are described in detail in Refs. [1,19–22]. The fourth detector (LaBr$_3$:Ce) with dimensions of 7.62 cm $\times$ 7.62 cm, was placed at about 30 degrees relative to the neutron-beam axis and 60 cm away from the fission source. A sketch of the experimental setup is shown in Fig. 1.

During the measurement, the signals from fission-fragments at both cathode and anode of each part of the ionization chamber as well as from each γ detector were recorded with digitizers with a sampling rate of 400 MS/s and 14 bit resolution [23]. Fission and coincidence trigger rates were recorded simultaneously with an *ORTEC 974 Counter/Timer* [24] to correct for dead time and for determining the prompt-γ-ray multiplicity (see below). During offline analysis each trace was checked for pileup and double hits. Within the maximum coincidence-time window of 50 ns no double hits were recorded. Double coincidences amounted to 0.06%. The cathode signal was used to determine the instant of fission, whereas the signal at the anode of the photomultipliers indicated the time of detection of a γ ray. The time difference of both signals is a measure of the time-of-flight (TOF) of a coincident event and enables us to discard all events that arrived later in time than expected from a prompt γ ray, e.g., due to neutron-induced reactions other than fission. The signals from the photomultiplier anode were then converted into pulse height, which gives, after proper calibration with different γ sources, the energy deposited in the detector.
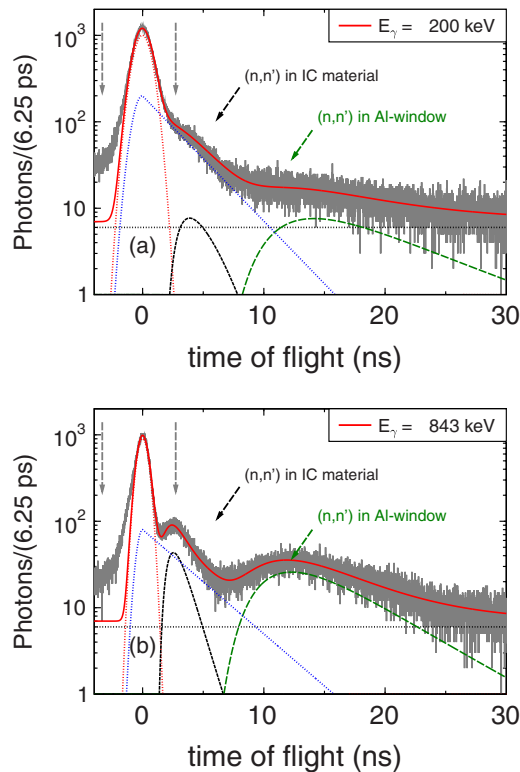
FIG. 2. (Color online) Time-of-flight (TOF) spectra for different γ-ray energies, (a) $E_\gamma = 200\,(5)$ keV and (b) $E_\gamma = 843\,(21)$ keV. The FWHM of the prompt-fission γ-ray peak is 1.65 (2) and 1.06 (2) ns, respectively. The dashed arrows indicate from which part of the TOF spectrum the prompt-fission γ-ray spectra were constructed. The full (red) lines illustrate the sum of the different components. For higher TOF values the presence of γ rays from isomer decay in fission fragments and inelastic scattering of prompt-fission neutrons in the detector material (^{27}Al, $E_\gamma = 843$ keV) and the ionization chamber (IC; ^{56}Fe, $E_\gamma = 846$ keV) is visible (dotted and dashed lines, respectively).

Typical TOF spectra for the LaBr$_3$:Ce (Q489) detector are depicted in Fig. 2, taken for two different γ-ray-energy cuts, $E_\gamma = 200\,(5)$ and 843 (21) keV, respectively. The width of each cut corresponds to the full width at half maximum (FWHM) energy resolution of the detector at this γ-ray energy. The coincidence-timing resolution, i.e., the FWHM of the prompt-fission γ-ray peak, is 1.65 (2) and 1.06 (2) ns, respectively. Assuming a timing resolution of $\delta t = 0.96$ ns (FWHM) for the ionization chamber, the corresponding values for the LaBr$_3$:Ce (Q489) are $\delta t = 1.2$ and 0.45 ns (FWHM), respectively, which are expected at those γ-ray energies for a 5.08 cm × 5.08 cm LaBr$_3$:Ce crystal coupled to a photomultiplier which is optimized for energy resolution. The TOF range for prompt-fission γ rays is indicated by the dashed vertical arrows and corresponds to less than $\Delta t = \pm 3$ ns. The full (red) lines illustrate the sum of the different components identified in the TOF spectrum. γ rays from isomer decay in fission fragments and from inelastic scattering of prompt-fission neutrons in the detector material are depicted with dotted and dashed lines, respectively. From this illustration it is obvious that the

contribution from inelastic prompt-fission neutron scattering is suppressed to a negligible fraction. The contribution from inelastic scattering of prompt-fission neutrons on ^{56}Fe, present in the ionization chamber (IC) was subtracted from the prompt-fission γ-ray spectrum. The horizontal (dotted) line in Fig. 2 indicates random coincidences. This contribution has been taken for a time region sufficiently far away from the prompt region, properly normalized and subtracted from the prompt spectrum.

About 50% of the decay γ rays from short-lived isomers, with an average half-life $t_{1/2} \approx 1.5$ ns, are included in our PFGS data. Decay γ rays from longer-lived isomers fall mainly outside the defined region. A more detailed analysis of isomeric γ rays in correlation with the coincident fission-fragment kinetic energy will be the subject of a forthcoming presentation.

In order to deduce the emitted prompt-fission γ-ray spectrum, the measured spectra have to be corrected with the response function of each detector. These response functions were determined by means of Monte Carlo simulations with the PENELOPE2011 computer code [26], folded with the energy resolution of the corresponding detectors and taking into account the actual geometry as well as the total number of fission events. In Ref. [1], this as well as the actual extraction of the emission spectrum are described in detail, which is the reason why we restrict ourselves here to present only the resulting emission spectra and their characteristics, as done below.

III. RESULTS AND DISCUSSION

According to the procedure sketched above, prompt-fission γ-ray spectra were obtained from the data taken with four different detectors. They are depicted in the upper part of Fig. 3, where the labels indicate both the respective scintillator crystal and detector number. All energy distributions exhibit very good agreement with respect to both shape and absolute value over the entire energy region up to 6 MeV, as indicated by the error bars, which for the sake of clarity are shown only for one detector (Q489). These point-wise error bars contain statistical uncertainties as well as contributions from the Monte Carlo simulations, the unfolding procedure, as well as all other data treatment. The lower part of Fig. 3 shows an enhanced view on the low-energy part of the spectra above, exhibiting a distinct structure of discrete γ peaks. According to, e.g., Ref. [15], these peaks are due to deexcitations of secondary fission fragments along the yrast bands, taking place after the statistical part of dipole transitions, which leads to a continuous γ spectrum. This peak structure appears in all four spectra, despite the slightly different energy resolution of the detectors, which is reflected in the widths of the respective peaks. The agreement of the peak positions is excellent, hence confirming that the energy calibration was performed correctly for all detectors. Also shown there is the evaluated data from ENDF/B-VII.1 [13]. Although the evaluation is in relatively good agreement with our data, it systematically underestimates the photon yield below 600 keV and does not show any structure; cf. Fig. 3(b).
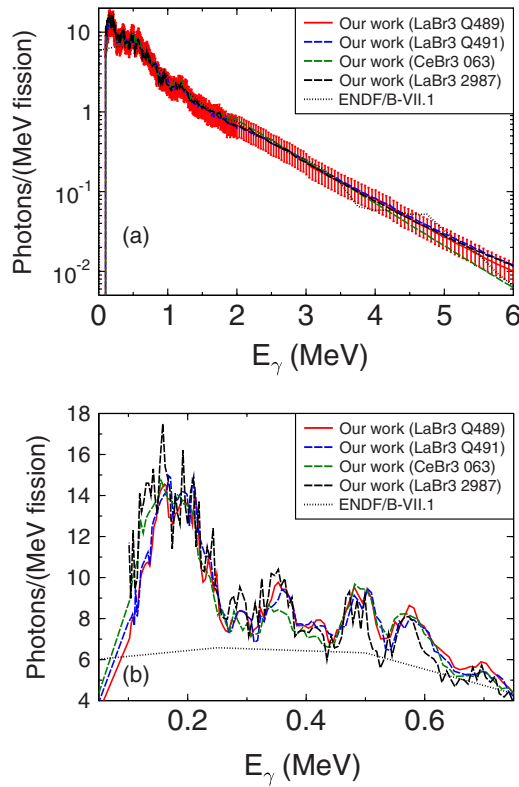
FIG. 3. (Color online) (a) The prompt-fission γ-ray emission spectrum for the thermal-neutron-induced fission on ^{241}Pu taken with four lanthanide-halide detectors. All spectra agree very well with each other. Here, the point-wise uncertainty is given only for detector Q489 for the sake of clarity. (b) The low-energy part of the spectrum reveals the differences to the recent ENDF/B-VII.1 evaluation [13].

Characteristic parameters for prompt-fission γ-ray emission, like the average number of photons per fission, $\overline{\nu}_\gamma$, as well as mean and total energy, ϵ_γ and $E_{\gamma,\mathrm{tot}}$, were obtained according to

$$\overline{\nu}_\gamma = \int N_\gamma(E_\gamma) dE_\gamma, \qquad (1)$$

$$E_{\gamma,\mathrm{tot}} = \int E_\gamma N_\gamma(E_\gamma) dE_\gamma, \qquad (2)$$

$$\epsilon_\gamma = E_{\gamma,\mathrm{tot}} / \overline{\nu}_\gamma, \qquad (3)$$

with $N_\gamma(E_\gamma)$ denoting the spectra depicted in Fig. 3(a). The lower limit was chosen to be 100 keV for all detectors, since the low-energy thresholds in this experiment were just below. The upper limit was 6 MeV, which was the maximum energy measured with sufficient statistics. The characteristic parameters were determined for each detector by replacing the integrals above by sums, and average values, weighted with the individual uncertainties, were calculated. All results are summarized in Table II, where they are compared with experimental results from Ref. [25] as well as with data from the evaluated library ENDF/B-VII.1 [13]. The results are also shown in Fig. 4, where the symbols denote the individual values, while mean values and their uncertainties are indicated by full drawn and dashed lines, respectively. From a previous
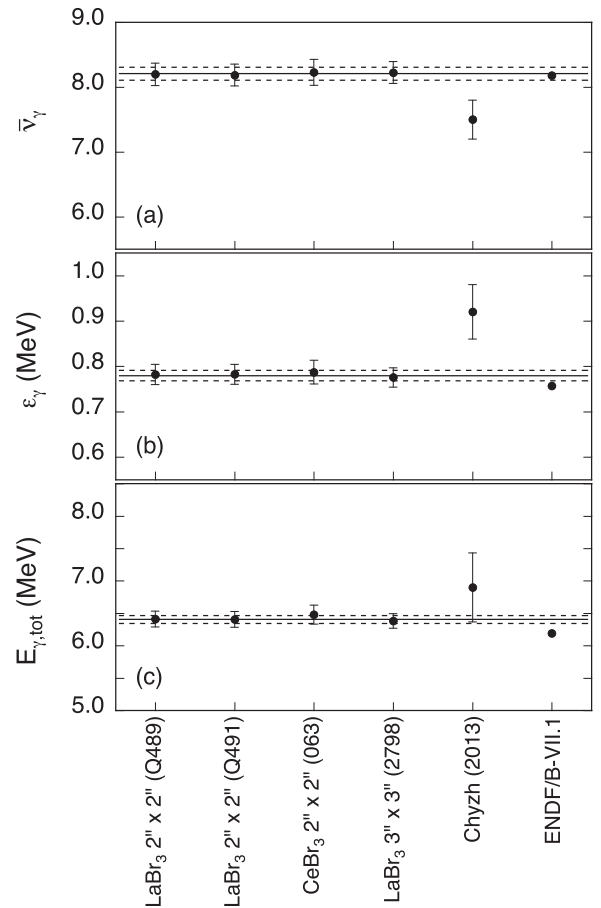

FIG. 4. Overview of results for the measurement of prompt-γ-ray emission for the neutron-induced fission of ^{241}Pu: (a) Average photon multiplicity, (b) mean photon energy per fission, and (c) total released photon energy from this work are compared with values from ENDF/B-VII.1 [13] as well as to recent data from Ref. [25] Values averaged over the results obtained with all four detectors and their uncertainties are displayed as full drawn and dashed lines, respectively.

study of ours [2], we know that the error introduced by integrating only up to 6 MeV is—at most—of the order of the uncertainty after averaging over all four detectors and has, therefore, been neglected.

From this comparison it is obvious that the results reported in Ref. [25], obtained with epithermal neutrons, differ considerably from all other values, i.e., the γ-ray multiplicity is too low, while the mean energy per photon is too high. This is not surprising because, although a low-energy threshold of 150 keV is quoted by the authors, a strong spectrum attenuation is visible below 400 keV. This leads to the observed lower multiplicity and higher mean energy per emitted photon. As a consequence, the total γ-ray energy is overestimated by 7.6% compared with our value. The present data in ENDF/B-VII.1 [13] shows slightly lower multiplicity and mean energy per photon, resulting in an underestimation of the average total γ-ray energy by 3.5%.

TABLE II. Summary of prompt-γ-ray characteristics for the thermal-neutron-induced fission on ^{241}Pu. Experimental results from this work for the average γ-ray multiplicity $\overline{\nu}_\gamma$, the average energy ϵ_γ, and the total energy $E_{\gamma,\mathrm{tot}}$, obtained with all four detectors employed in this work, are given and the covered energy range is indicated. Averaged values for the four detectors are presented as well and compared with the evaluated nuclear data files in ENDF/B-VII.1 [13] and to recent data from Chyzh $et\ al.$ [25] obtained from epithermal-neutron-induced fission. The uncertainties on their mean values, denoted by *), were estimated from uncertainties discussed there.

Results	Detector	Diameter × length (cm × cm)	$\overline{\nu}_\gamma$ (per fission)	ϵ_γ (MeV)	$E_{\gamma,\mathrm{tot}}$ (MeV)	Energy range (MeV)
This work	LaBr$_3$:Ce (Q489)	5.08 × 5.08	8.20 ± 0.17	0.78 ± 0.02	6.41 ± 0.12	0.1–6.0
This work	LaBr$_3$:Ce (Q491)	5.08 × 5.08	8.19 ± 0.17	0.78 ± 0.02	6.41 ± 0.12	0.1–6.0
This work	CeBr$_3$ (063)	5.08 × 5.08	8.23 ± 0.20	0.79 ± 0.03	6.48 ± 0.15	0.1–6.0
This work	LaBr$_3$:Ce (2789)	7.62 × 7.62	8.23 ± 0.17	0.78 ± 0.02	6.38 ± 0.11	0.1–6.0
This work	Averaged values		8.21 ± 0.09	0.78 ± 0.01	6.41 ± 0.06	0.1–6.0
ENDF/B-VII.1 [13]	Evaluation		8.18	0.76	6.19	0.1–10.0
Chyzh $et\ al.$ [25]	DANCE (BaF$_2$)		7.5 ± 0.3 *)	0.92 ± 0.06 *)	6.90 ± 0.53 *)	0.15–9.5

IV. CONCLUSIONS

In this work we reported on the measurement of prompt-fission γ-ray spectra (PFGS) from the reaction $n_{\mathrm{th}} + {}^{241}$Pu. Different lanthanide halide scintillation detectors were employed and have proven again (cf. Refs. [1,2]) that they constitute a well-suited choice of instrumentation for this kind of investigation. PFGS characteristics were determined with high precision. Our results are $\overline{\nu}_\gamma = (8.21 \pm 0.09)$ per fission, $\epsilon_\gamma = (0.78 \pm 0.01)$ MeV, and $E_{\gamma,\mathrm{tot}} = (6.41 \pm 0.06)$ MeV. The achieved uncertainty of 0.9% for the mean total γ-ray energy is well below the requested uncertainty of 7.5% at most with respect to the γ heating in advanced nuclear reactor core simulations [8–10]. This achievement was possible due to the excellent agreement between the emission spectra obtained with each of our detectors, which allowed us to average the individual results in order to reduce the uncertainties.

Based on the new data we recommend an update of the evaluated data file of PFGS for ^{241}Pu, although the average total prompt-fission γ-ray energy given there underestimates our results by not much; see Fig. 4(c). Hence, the observed γ-heat excess might be accounted for not only by thermal-neutron-induced fission, but alternative explanations could be necessary. For instance, fast-neutron-induced fission, in particular on ^{238}U, could be contributing, which is a strong motivation for us to investigate its PFGS in the near future. One may also suspect a non-negligible contribution to the γ heating from fission induced by γ rays emitted after neutron capture in the construction material.

[1] R. Billnert, F.-J. Hambsch, A. Oberstedt, and S. Oberstedt, Phys. Rev. C **87**, 024601 (2013).

[2] A. Oberstedt, T. Belgya, R. Billnert, R. Borcea, T. Bryś, W. Geerts, A. Göök, F.-J. Hambsch, Z. Kis, T. Martinez, S. Oberstedt, L. Szentmiklosi, K. Takàcs, and M. Vidali, Phys. Rev. C **87**, 051602(R) (2013).

[3] A. Chyzh, C. Y. Wu, E. Kwan, R. A. Henderson, J. M. Gostic, T. A. Bredeweg, R. C. Haight, A. C. Hayes-Sterbenz, M. Jandel, J. M. O'Donnell, and J. L. Ullmann, Phys. Rev. C **85**, 021601(R) (2012).

[4] V. V. Verbinski, H. Weber, and R. E. Sund, Phys. Rev. C **7**, 1173 (1973).

[5] F. Pleasonton, R. L. Ferguson, and H. W. Schmitt, Phys. Rev. C **6**, 1023 (1972).

[6] R. W. Peelle and F. C. Maienschein, Phys. Rev. C **3**, 373 (1971).

[7] Nuclear Data High Priority Request List of the NEA (Req. ID: H.3, H.4), http://www.nea.fr/html/dbdata/hprl/hprlview.pl?ID=421 and http://www.nea.fr/html/dbdata/hprl/hprlview.pl?ID=422

[8] G. Rimpault, A. Courcelle, and D. Blanchet, Comment to the HPRL: ID H.3 and H.4.

[9] G. Rimpault, D. Bernard, D. Blanchet, C. Vaglio-Gaudard, S. Ravaux, and A. Santamaria, Phys. Procedia **31**, 3 (2012).

[10] G. Rimpault, *Proceedings of International Workshop on Nuclear Data Needs For Generation IV Nuclear Energy Systems, April 2005*, edited by P. Rullhusen (World Scientific, Singapore, 2006).

[11] A. Lüthi, R. Chawla, and G. Rimpault, Nucl. Sci. Eng. **138**, 3 (2001).

[12] D. Blanchet, *Proceedings of M&C 2005 International Topical Meeting on Mathematics and Computation, Supercomputing, Reactor Physics and Nuclear and Biological Applications, Sept. 12–15, 2005, Palais Des Papes, Avignon, France* (CEA, France, available as CD).

[13] ENDF/B-VII.1 Evaluated Nuclear Data File ZA = 92235, MF = 15, MT = 18 (2011), http://www.nndc.bnl.gov/exfor/endf00.jsp

[14] D. Regnier, O. Litaize, and O. Serot, Phys. Procedia **47**, 47 (2013).

[15] O. Litaize and O. Serot, Phys. Rev. C **82**, 054616 (2010).

[16] P. Talou, T. Kawano, and I. Stetcu, Phys. Procedia **47**, 39 (2013).

[17] B. Becker, P. Talou, T. Kawano, Y. Danon, and I. Stetcu, Phys. Rev. C **87**, 014617 (2013).

[18] http://www.bnc.hu

[19] R. Billnert, E. Andreotti, F.-J. Hambsch, M. Hult, J. Karlsson, G. Marissens, A. Oberstedt, and S. Oberstedt, Phys. Procedia **31**, 29 (2012).

[20] A. Oberstedt, R. Billnert, and S. Oberstedt, Nucl. Instrum. Methods Phys. Res., Sect. A **708**, 7 (2013).

[21] R. Billnert, S. Oberstedt, E. Andreotti, M. Hult, G. Marissens, and A. Oberstedt, Nucl. Instrum. Methods Phys. Res., Sect. A **647**, 94 (2011).

[22] G. Lutter, M. Hult, R. Billnert, A. Oberstedt, S. Oberstedt, E. Andreotti, G. Marissens, U. Rosengård, and F. Tzika, Nucl. Instrum. Methods Phys. Res., Sect. A **703**, 158 (2013).

[23] http://spdevices.com/index.php/adq214

[24] http://www.ortec-online.com/Solutions/modular-electronic-instruments.aspx

[25] A. Chyzh, C. Y. Wu, E. Kwan, R. A. Henderson, J. M. Gostic, T. A. Bredeweg, A. Couture, R. C. Haight, A. C. Hayes-Sterbenz, M. Jandel, H. Y. Lee, J. M. O'Donnell, and J. L. Ullmann, Phys. Rev. C **87**, 034620 (2013).

[26] http://www.oecd-nea.org/tools/abstract/detail/nea-1525